JOURNAL OF SOLID STATE CHEMISTRY 67, 9–20 (1987)

# X-Ray Study of the Second-Order Phase Transition of $Ag_{0.35}TiS_2$: A Phase Transition Characterized by Two Order Parameters

G. A. WIEGERS,* K. D. BRONSEMA,† S. VAN SMAALEN,‡
R. J. HAANGE, J. E. ZONDAG, AND J. L. DE BOER

*Laboratory of Inorganic Chemistry, Materials Science Center, University of Groningen, Nijenborgh 16, 9747 AG Groningen, The Netherlands*

Received January 23, 1986; in revised form May 23, 1986

$Ag_{0.35}TiS_2$ shows a second-order phase transition with $T_c$ = 298.0 K from a $a\sqrt{3} \times a\sqrt{3} \times 2c$ superstructure, space group $P\bar{3}1c$, to a disordered $Cd(OH)_2$–NiAs intermediate structure with unit cell $a \times a \times c$ and space group $P\bar{3}m1$. In the disordered structure silver atoms occupy fractionally the sites of triangular lattice planes. Below $T_c$ silver atoms occupy special sites in space group $P\bar{3}1c$: Ag($\alpha$) at $\pm(0, 0, \frac{1}{4})$, Ag($\beta$) at $\pm(\frac{2}{3}, \frac{1}{3}, \frac{1}{4})$, and Ag($\gamma$) at $\pm(\frac{1}{3}, \frac{2}{3}, \frac{1}{4})$. The order is characterized by two order parameters $\eta_1 = n(\beta) - n(\gamma)$ and $\eta_2 = n(\beta) + n(\gamma) - 2n(\alpha)$, where $n(\alpha)$, $n(\beta)$, and $n(\gamma)$ are the occupancies of the $\alpha$, $\beta$, and $\gamma$ sites, respectively. Single-crystal X-ray diffraction of the ordered structure showed the occupancies $n(\alpha) = 0.172$, $n(\beta) = 0.861$, $n(\gamma) = 0$ at 100 K and $n(\alpha) = 0.180$, $n(\beta) = 0.786$, $n(\gamma) = 0.069$ at 255 K. Critical exponents $\beta_1$ and $\beta_2$ of the order parameters $\eta_1$ and $\eta_2$ were determined from the temperature dependence of the intensities of the superreflections 101 and 102, respectively; the values obtained, $\beta_1 = 0.41$ and $\beta_2 = 0.81$, are between those predicted by P. Bak (*Phys. Rev. Lett.* **44**, 889 (1980)) from scaling laws: $\beta_1 = 0.33$ and $\beta_2 = 0.86$, and from mean field theory: $\beta_1 = 0.5$, $\beta_2 = 1.0$. The temperature dependence of the order parameters in the temperature range 100–298 K is compared with that from a Bragg–Williams (mean field) model, the energy being written in terms of nearest-neighbor repulsive interactions, $\varepsilon_1$ for atoms at distance $a$ and $\varepsilon_2$ for atoms at distance $c$; $\varepsilon_1 > \varepsilon_2$ because $c > a$. The space group of the observed structure, $P\bar{3}1c$, is discussed in (3 + 1)D superspace, which gives an alternate description for the symmetry of this commensurately modulated phase. Finally, some related phases are discussed. 

## 1. Introduction

The disordered structure of $Ag_{0.35}TiS_2$ is of the intermediate $Cd(OH)_2$–NiAs structure ($a \times a \times c$ unit cell) with silver atoms in the octahedral sites between sulfur atoms of neighboring $TiS_2$ sandwiches; these sites, forming triangular lattice planes, are fractionally occupied, $\bar{n}$ = 0.35 (Fig. 1). This fractional occupation of lattice sites leaves the possibility of several types of order–disorder transitions: transformations with ordering in the lattice planes with no change in the average occupancy of the sites of each plane (intralayer order–disorder transitions) and transformations for which the average occupancy of the sites of each plane of silver changes (interlayer order–disorder transition). The latter is the case for stage transformations, e.g., a sec-

* To whom correspondence should be addressed.
† Present address: Enka B.V. Research Institute Arnhem, Velperweg 76, Arnhem, The Netherlands.
‡ Present address: Department of Physics and Chemistry, State University of New York at Buffalo, Amherst, New York 14260.



0022-4596/87 $3.00

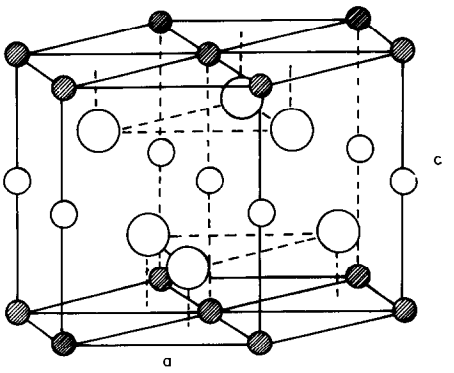


FIG. 1. Structure of disordered $Ag_{0.35}TiS_2$ is a perspective view. Small open and large open spheres are titanium and sulfur atoms, respectively; silver atoms are hatched.

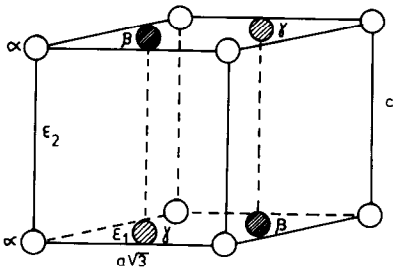


FIG. 3. The silver sublattice of the ordered structure in perspective view; the silver sites are indicated by $\alpha$, $\beta$, and $\gamma$; the nearest-neighbor repulsive interactions $\varepsilon_1$ and $\varepsilon_2$ are also indicated (see Sect. 6). Cell edges are in units of the disordered structure.

ond-stage phase (gaps between sandwiches alternating between fractionally occupied and empty) transforming into a first-stage phase with all gaps between sandwiches fractionally occupied. The transformation of our study is of the first type; the average occupancy of the lattice sites of each plane is not changed but silver atoms order on a $a\sqrt{3} \times a\sqrt{3} \times 2c$ lattice (*1–3*) (Figs. 2 and 3).

Two-dimensional (2D) order only of silver atoms on a $a\sqrt{3} \times a\sqrt{3}$ lattice has been observed for stage-2 $Ag_{0.18}TiS_2$ with $\bar{n}$ = 0.36 (*4–6*). In this stage-2 phase, planes of silver are at distances of 12.12 Å, which is about twice the distance (6.398 Å) between silver planes of stage-1 $Ag_{0.35}TiS_2$.

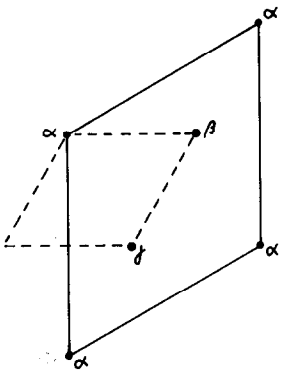


FIG. 2. The *ab* plane of the unit cell of the disordered (dashed lines) and the ordered (full lines) structure of $Ag_{0.35}TiS_2$. The $\alpha$, $\beta$, and $\gamma$ sites of silver at $z = \frac{1}{4}$ are indicated.

In a previous paper (*3*) we reported the structure determination of the disordered and the ordered phase $Ag_{0.35}TiS_2$ at temperatures of 300 and 100 K, respectively, as well as the electrochemical and thermodynamic properties of intercalates $Ag_xTiS_2$. AC response and GITT (galvanostatic intermittent titration technique) at temperature above about 450 K showed the stage-2 phase ($0.18 \leq x \leq 0.22$) and stage-1 phase ($0.36 \leq x \leq 0.44$) to be superionic conductors (*3*). The phases show a metallic type of electronic conduction which will be described in a forthcoming paper.

The order–disorder transition of stage-1 $Ag_xTiS_2$ has been the subject of several studies. Suter *et al.* (*2*) studied the transition of $Ag_{0.33}TiS_2$ crystals prepared from the elements by measuring the intensity and the excess linewidth of a superreflection of the $a\sqrt{3} \times a\sqrt{3} \times 2c$ supercell as a function of temperature. They found the transition to be of second-order nature, $T_c$ being 250 K. Raman scattering experiments by Lionelli *et al.* (*7*) revealed the occurrence of a continuous transition, with $T_c$ = 300 K. Two-dimensional order of silver in stage-2 $Ag_{0.18}TiS_2$ was analyzed by Oshima and

Moss (*6*) from the diffuse X-ray scattering.

In this paper we report on the nature of the order–disorder transition of stage-1 $Ag_{0.35}TiS_2$. In Section 2 we describe the structure determination of the ordered phase at 255 and 100 K. The structures are discussed in Section 3. The determination of the critical exponents of the two order parameters $\eta_1$, and $\eta_2$ is described in Section 4. In Section 5 the determination of the order parameters in the range 100–300 K is described. The results are compared with those from a mean field model in Section 6. The ordered structure using (3 + 1)D superspace is explained in Section 7. Some related phases are discussed in Section 8.

## 2. X-Ray Diffraction

Experimental details concerning the preparation of single crystals have been described in our previous paper (*3*). Weissenberg photographs taken at room temperature of a single crystal aligned along the *a*-axis revealed the presence of superreflections due to a $a\sqrt{3} \times a\sqrt{3} \times 2c$ supercell. Besides these superreflections, diffuse scattering is also visible. This scattering is along c* and concentrated around the superreflections, which indicates that short-range order is mainly in the planes of silver, the correlation between neighbor planes of silver being small. It also appeared that superreflections (the extra reflections besides those of the subcell) with $L$ odd are stronger than those with $L$ even. In the following we will use capitals $HKL$ for the indices of the reflections in the $a\sqrt{3} \times a\sqrt{3} \times 2c$ supercell. We adopted space group $P\bar{3}1c$ for which the extinction rule is: reflections $HHL$ with $L$ odd not present. These reflections were not visible on Weissenberg photographs. This space group will be discussed in relation with symmetry in (3 + 1)D superspace in Section 7.

In $P\bar{3}1c$ the atoms are on positions given in Table I. Titanium and silver atoms are on special positions; the silver sites are designated as Ag($\alpha$) (at 2*a*: $\pm(0, 0, \frac{1}{4})$), Ag($\beta$) (at 2*c*: $\pm(\frac{2}{3}, \frac{1}{3}, \frac{1}{4})$), and Ag($\gamma$) at 2*d*: $\pm(\frac{1}{3}, \frac{2}{3}, \frac{1}{4})$. The silver sublattice is shown in Fig. 3.

TABLE I

ATOMIC POSITIONS OF THE ATOMS OF $Ag_{0.35}TiS_2$ IN SPACE GROUP $P\bar{3}1c$

| Atom | Site | Site symmetry | Coordinate |
|---|---|---|---|
| S | 12*i* * | 1 | $\pm(x, y, z)$, . . . ; $z \approx \frac{1}{8}$, $y \approx 0$, $z \approx z'/2$ |
| Ti(1) | 2*b* | $\bar{3}$ | 0, 0, 0; 0, 0, $\frac{1}{2}$ |
| Ti(2) | 4*f* | 3 | $\pm(\frac{1}{3}, \frac{2}{3}, z)$; $\pm(\frac{1}{3}, \frac{2}{3}, \frac{1}{2} - z)$; $z \approx 0$ |
| Ag($\alpha$) | 2*a* | 32 | $\pm(0, 0, \frac{1}{4})$ |
| Ag($\beta$) | 2*c* | 32 | $\pm(\frac{2}{3}, \frac{1}{3}, \frac{1}{4})$ |
| Ag($\gamma$) | 2*d* | 32 | $\pm(\frac{1}{3}, \frac{2}{3}, \frac{1}{4})$ |

*Note.* $z'$ is the coordinate of sulfur in the disordered structure (Table II).

Weissenberg photographs taken at 100 K showed that the diffuse scattering has disappeared, superreflections with $L$ odd being stronger than those with $L$ even. This observation is obvious considering the structure factor of the superreflections. Ignoring the contributions from sulfur and Ti(1) (which are small), the geometrical part of the structure factor is given by

$$|F| = \sqrt{3}\,[n(\beta) - n(\gamma)]$$

for superreflections with L odd,

$$|F| = n(\beta) + n(\gamma) - 2n(\alpha)$$

for superreflections with L even.

Weissenberg photographs taken at temperatures in the range 250–320 K proved the continuous character of the transition. The transition is due to ordering of silver atoms, the $\beta$ site being occupied at the expense of the $\alpha$ and $\gamma$ sites. It may be noted that instead of the $\beta$ site the $\gamma$ site may be taken as well as the occupied site below $T_c$. It is convenient to take the parameters describing the order as

$$\eta_1 = n(\beta) - n(\gamma)$$

$$\eta_2 = n(\beta) + n(\gamma) - 2n(\alpha).$$

In this case the intensities of the super-

TABLE II

ATOMIC COORDINATES, OCCUPANCIES, AND THERMAL PARAMETERS OF THE DISORDERED STRUCTURE OF $Ag_{0.35}TiS_2$ AT 300 K

| Atom | Occupancy | Coordinate | $U(11)$ (100 Å) | $U(33)$ (100 Å) |
|---|---|---|---|---|
| S | 1 | $\pm(\frac{1}{3}, \frac{2}{3}, 0.2231(4))$ | 0.81(3) | 1.57(6) |
| Ti | 1 | 0, 0, 0 | 0.92(3) | 1.76(6) |
| Ag | 0.346(5) | 0, 0, $\frac{1}{2}$ | 3.11(9) | 1.43(5) |

*Note.* $a$ = 3.4275(6) Å, $c$ = 6. 3977(7) Å, space group $P\bar{3}m1$. The temperature factor has the form

$$T = \exp - 2\pi^2 \sum_{i,j} h_i k_j a_i^* a_j^* U(i, j).$$

Standard deviations in the last decimal place are given in parentheses.

reflections with $L$ odd and even are proportional to $\eta_1^2$ and $\eta_2^2$, respectively.

The intensities of the reflections were measured at 255 and 100 K. Our data, covering reflections up to $\sin\theta/\lambda$ = 1.407 Å, were measured on a CAD-4F kappa diffractometer (Enraf–Nonius) using monochromatized Mo$K\alpha$ radiation. Use was made of the $\omega$ scan technique. The crystal was cooled with a stream of evaporating liquid nitrogen. The temperature during each intensity measurement was measured and stored (*8*). Reflections with $-15 \leq H \leq 8$, $0 \leq K \leq 15$, and $0 \leq L \leq 33$ were measured. The intensities were corrected for Lorentz polarization and absorption (*9*). Inspection of the intensities of 4958 measured intensities showed that the Laue group is $\bar{3}m$: after averaging over equivalent reflections the intensities of 2060 independent reflections with $I > 3\sigma(I)$ at 100 K and 1503 independent reflections with $I > 3\sigma(I)$ at 255 K were available.

Refinements were carried out using the X-ray system (*10*); scattering factors were those from Cromer and Mann (*11*). The refinements converged smoothly to $R_F$ = 0.039 for data measured at 100 K and to $R_F$ = 0.055 for those at 255 K. Results of the superstructure at 300 K, already mentioned in our previous paper, are given in Table II for comparison with the refinement results in Tables III and IV.

## 3. Discussion of the Structure

The refinement of the substructure (at 300 K) confirmed the proposed structure from powder data (*1*). Ag and Ti are in trigonally distorted octahedra of sulfur atoms, the Ag–S and Ti–S distances being 2.656 and 2.440 Å, respectively. The average occupancy $\bar{n}$ of the silver site is 0.345. An interesting feature is the large anisotropy of the thermal motion of silver, $\langle u_{ab}^2 \rangle^{1/2}$, the root-mean-square amplitude of vibration in the $ab$ plane being much larger than $\langle u_c^2 \rangle^{1/2}$, the rms amplitude along $c$. The latter ampli-

TABLE III

ATOMIC COORDINATES, OCCUPANCIES, AND THERMAL PARAMETERS OF THE ATOMS IN THE ORDERED STRUCTURE OF $Ag_{0.35}TiS_2$ AT 100 K

| Atom | Occupancy | $x$ | $y$ | $z$ | $U(11)$ (100 Å$^2$) | $U(22)$ (100 Å$^2$) | $U(33)$ (100 Å$^2$) |
|---|---|---|---|---|---|---|---|
| S | 1 | .32934(7) | −.00506(7) | .11217(2) | .327(9) | .312(9) | .513(8) |
| Ti(1) | 1 | 0 | 0 | 0 | .302(8) | | .601(14) |
| Ti(2) | 1 | $\frac{1}{3}$ | $\frac{2}{3}$ | .00004(5) | .339(6) | | .571(9) |
| Ag($\alpha$) | .171(2) | 0 | 0 | $\frac{1}{4}$ | 1.48(4) | | .32(4) |
| Ag($\beta$) | .861(3) | $\frac{2}{3}$ | $\frac{2}{3}$ | $\frac{1}{4}$ | 1.029(7) | | .474(7) |
| Ag($\gamma$) | 0 | $\frac{1}{3}$ | $\frac{1}{3}$ | $\frac{1}{4}$ | — | | — |

*Note.* $a$ = 5.9288(7) Å, $c$ = 12.744(9) Å, space group $P\bar{3}1c$. Temperature factor of the form given in Table II. Nondiagonal tensor elements of the temperature factor of sulfur: $U(12)$ = .167(7), $U(13)$ = −.04(7), $U(23)$ = −.035(7) Å$^2$. Tensor elements $U(ij)$ are multiplied by 100.

TABLE IV

ATOMIC COORDINATES, OCCUPANCIES, AND THERMAL PARAMETERS OF THE ATOMS IN THE ORDERED STRUCTURES OF $Ag_{0.35}TiS_2$ AT 255 K

| Atom | Occupancy | $x$ | $y$ | $z$ | $U(11)$ (100 Å$^2$) | $U(22)$ (100 Å$^2$) | $U(33)$ (100 Å$^2$) |
|---|---|---|---|---|---|---|---|
| S | 1 | .3301(1) | −.00414(10) | .1164(4) | .72(2) | 0.68(2) | 1.08(2) |
| Ti(1) | 1 | 0 | 0 | 0 | .81(1) | | 1.30(3) |
| Ti(2) | 1 | $\frac{1}{3}$ | $\frac{2}{3}$ | .0002(4) | .85(1) | | 1.30(2) |
| Ag($\alpha$) | .180(3) | 0 | 0 | $\frac{1}{4}$ | 3.9(1) | | .96(5) |
| Ag($\beta$) | .786(3) | $\frac{2}{3}$ | $\frac{1}{3}$ | $\frac{1}{4}$ | 2.48(2) | | .99(2) |
| Ag($\gamma$) | .064(3) | $\frac{1}{3}$ | $\frac{2}{3}$ | $\frac{1}{4}$ | 2.4(2) | | 1.2(1) |

*Note.* $a$ = 5.9424(6), $c$ = 12.791(8) Å, space group $P\bar{3}1c$. Temperature factor of the form given in Table II. Nondiagonal tensor elements of the temperature factor of sulfur: $U(1,2)$ = 0.35(1), $U(13)$ = −0.05(1), $U(23)$ = −0.05(1) Å$^2$. Tensor elements are multiplied by 100.

tude is about the same as $\langle u_{ab}^2 \rangle^{1/2}$, and $\langle u_c^2 \rangle^{1/2}$ of titanium and sulfur. Such an anisotropy in the thermal motion of silver was also found in $Ag_{0.18}TiS_2$ (*6*), $Ag_{0.67}NbS_2$ (*12*), and $AgCrS_2$ (*12*), the latter two compounds having silver atoms in tetrahedral coordination by sulfur. The role of the thermal motion in relation with order–disorder transitions and the mechanism of fast-ion conduction will be the subject of a forthcoming paper.

X-Ray diffraction experiments are now being performed in order to trace the distribution of silver at higher temperatures: hopping versus liquid-like type of motion, and the possibility of the occupation of other sites in the planes of silver, e.g., the tetrahedral sites.

The occupancies $n(\alpha)$ = 0.172(2), $n(\beta)$ = 0.861(3), $n(\gamma)$ = 0, and $\bar{n}$ = 0.345 at 100 K (standard deviations in parentheses) are in agreement with those ($n(\alpha)$ = 0.14, $n(\beta)$ = 0.90, and $n(\gamma)$ = 0) of the experiment described in our previous paper (*3*), taking into account that the experiments described here cover a larger data set. At 255 K we found an intermediate distribution: $n(\alpha)$ = 0.180(3), $n(\beta)$ = 0.786(3), $n(\gamma)$ = 0.069(3), $\bar{n}$ = 0.343.

The coordinates of sulfur in the average structure (00$z$) transforms into $\frac{1}{3}$, 0, $\frac{z}{2}$ of the superstructure. The coordinates from the refinement significantly deviate from this value (Tables III and IV). We may consider this as a relaxation of the sulfur sublattice to the different occupancies of the $\alpha$, $\beta$, and $\gamma$ sites of silver, the distances of these sites to the neighboring sulfur atoms being 2.6377(5) Å, 2.6642(5) Å, and 2.6262(5) Å, respectively. The differences between these distances with respect to the average value are created by displacements of sulfur within the *ab* planes, the sulfur–sulfur distances being 3.4695(7) Å, 3.4083(10) Å, and 3.3917(9) Å (Figs. 4a and b), which may be compared with the S–S distance of 3.4230(5) Å in the disordered structure.

Ti(1) has site symmetry $\bar{3}$ and the Ti(1)–S distances are 2.4322(5) Å. The site symmetry of Ti(2) is 3 and there are two different Ti(2)–S distances, viz., 2.4601(4) Å (the three sulfur atoms also bonded to Ag($\beta$)) and 2.4252(5) Å (to sulfur atoms neighboring the unoccupied silver site) (Fig. 4b).

## 4. Critical Exponents of the Order Parameters

Our X-ray measurements described in Section 2 clearly showed the continuous character of the order–disorder transition. The possibility of second-order transitions between phases with $Cd(OH)_2$ type sub-

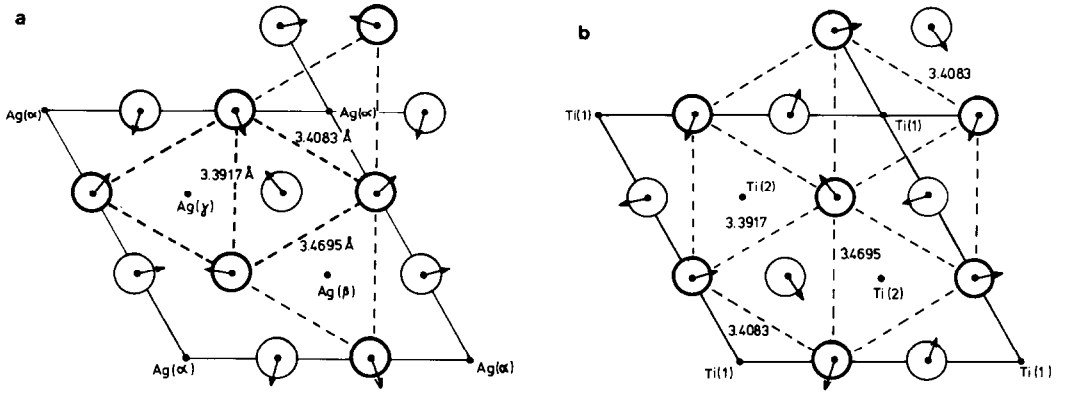


FIG. 4. (a) The sulfur atoms at $z = \frac{1}{8}$ (thin-lined circles) and $z = \frac{3}{8}$ (bold-lined circles) coordinating Ag at $z = \frac{1}{4}$ in the ordered structure. The arrows indicate the displacements from the positions in the average structure (relative scale). (b) The sulfur atoms at $z = -\frac{1}{8}$ (thin-lined circles) and $z = \frac{1}{8}$ (bold-lined circles) coordinating Ti atoms at $z = 0$ in the ordered structure. Displacements indicated as in (a).

structure was discussed on the basis of the Landau theory by Haas (*13*). For compounds like trigonal $Cr_2S_3$ and $Cr_5S_6$ with $a\sqrt{3} \times a\sqrt{3} \times 2c$ type superstructure, space group $P\bar{3}1c$, isostructural with $Ag_{0.35}TiS_2$ (to be discussed in Sect. 8), he then reported that a single second-order transition to the $a \times a \times c$ substructure, space group $P\bar{3}m1$, is not allowed. A reconsideration of this problem by Haas (*14*) has shown that the analysis given in (*13*) is wrong and that the Landau theory allows a second-order type transition between the ordered and the disordered structure.

The transition of $Ag_{0.35}TiS_2$ is characterized by order parameters $\eta_1$ and $\eta_2$ defined in Section 2. Systems closely related to ours, the intercalates of graphite, $EuC_6$, $YbC_6$, and $BaC_6$, have been discussed by Bak (*15*) in relation to possible continuous transitions. The disordered structure of these compounds has space group $P6_3/mmc$ while the structures of the metal sublattice in the ordered and disordered structure are the same as the silver sublattices in ordered and disordered $Ag_{0.35}TiS_2$. Bak predicts, on the basis of the Landau theory, a second-order order–disorder transition for the graphite intercalates. He also applied the theory of critical phenomena to the possible (experimentally not yet found) order–disorder transitions of these compounds.

According to the theory of critical phenomena the critical exponents $\beta$ of the order parameters $\eta$ of a second-order phase transition ($\eta \sim (1 - T/T_c)^{\beta}$) for a system with short-range interactions depend only on the spatial dimensionality and the number of independent components of the order parameter. For the Ising model of spins on a square lattice with ferromagnetic nearest-neighbor interactions, for example, the spatial dimensionality $D = 2$ and the order is characterized by a single ($d = 1$) order parameter $\eta \sim \langle M \rangle$, the magnetization, the critical exponent of $\eta$ being $\frac{1}{8}$. In the case of $D = 3$ the critical exponent for the Ising model is 0.312. Magnetic systems with higher dimensionality of the order parameter are the 3D-$XY$ (planar Heisenberg model ($d = 2$) and the 3D Heisenberg model ($d = 3$).

The order–disorder transition of the graphite intercalates discussed by Bak (*15*) as well as $Ag_{0.35}TiS_2$ of this study are described by two order parameters. The critical behavior is expected to be the same as for the 3D-$XY$ magnetic transition with $\beta_1$

of the primary order parameter $\eta_1$ equal to 0.33 and $\beta_2$, the exponent of $\eta_2$, being 0.86. One expects therefore that the intensities of superreflections with $L$ odd will be proportional to $(T_c - T)^{0.66}$ while the intensities for those with $L$ even will be proportional to $(T_c - T)^{1.72}$.

In Section 6 we will give a mean field model which shows the physical origin of the different temperature dependencies of the two order parameters. In the following we will discuss the determination of the critical exponents.

In order to determine the critical exponents in the case of $Ag_{0.35}TiS_2$, the intensities of the superreflections 101 and 102 were measured in the temperature range 260–300 K. Use was made of the $\omega$ scan technique in order to eliminate the contribution of the diffuse scattering in the measurement of the background intensities. Counting times of 30 sec for 101 and 75 sec for 102 were used; different counting times were chosen in order to obtain about the same number of counts (and therefore the same standard deviation) for the intensities of 101 and 102. The crystal, which was enclosed in a glass capillary, was cooled with a stream of nitrogen gas. The temperature was measured at a distance of about 0.5 cm from the crystal. The temperature variation during a measurement was about ±0.1 K; measurements with a larger variation were rejected. The variation in temperature is due to irregularities in the evaporation of liquid nitrogen used in temperature control. Several runs with increasing and decreasing temperature were performed. During a run the intensities at different temperatures were measured with time intervals of about 3 min; in most cases the measurements at the same temperature were repeated.

Log $I$ (intensity in counts) versus log $(T_c - T)$ plots were made in order to determine $2\beta_1$ (from 101) and $2\beta_2$ (from 102) as well as $T_c$. The results are shown in Fig. 5. We found $\beta_1 = 0.41 \pm 0.02$, $\beta_2 = 0.81 \pm 0.02$, $T_c = 298.0$ K. It is seen that the data points from measurements with increasing temperature (+) lie above those measured with decreasing temperature (·) which is probably due to a systematic error in the measurement of the temperature.

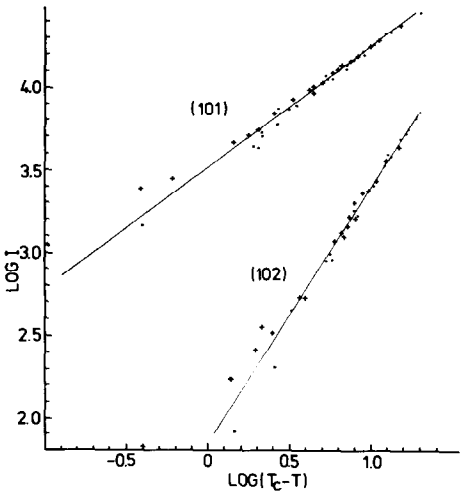


FIG. 5. Log $I$ (intensity in counts) versus log $(T_c - T)$ plots for the 101 and 102 superreflections. (+), Measurements with increasing temperature; (·), with decreasing temperature.

The values obtained for $\beta_1$ and $\beta_2$ compared to those predicted by Bak (*15*) (0.33 and 0.86, respectively) indicate that forces with longer range than nearest neighbors have to be taken into account. We will discuss this in Section 6.

## 5. Measurement of $\eta_1$ and $\eta_2$ in the Temperature Range 100–300 K

The power law $\eta \sim (T_c - T)^{\beta}$ describes the transition in the temperature region close to $T_c$. In order to determine $\eta_1$ and $\eta_2$ in the range down to 100 K the intensities of a number of superreflections with $L$ odd and $L$ even together with some subcell reflections were measured at temperatures of 207, 225, 239, 259, 272, 283, and 290 K. Below 207 K the relative change in intensity with temperature was the same for super- and subcell reflections; these changes were small and can be attributed to the de-

crease of the temperature factor only. We therefore assumed that already, at about 200 K, the occupancies of the silver sites are equal to those found at 100 K. The intensities of reflections with $L$ odd and even were scaled with respect to those at 207 K. From the square root of these relative values, proportional to

$$\frac{n(\beta) - n(\gamma)}{0.861} \quad \text{and} \quad \frac{1/2[n(\beta) + n(\gamma)] - n(\alpha)}{0.255}$$

for reflections with $L$ odd and even, respectively, and the relation $n(\alpha) + n(\beta) + n(\gamma) = 1.035$, it is possible to calculate $n(\alpha)$, $n(\beta)$, and $n(\gamma)$ for each temperature. The occupancies obtained are given in Fig. 6 together with those from a refinement at 255 K. In Fig. 7 a plot of $\eta_1$ and $\eta_2$ versus $T/T_c$ is given.

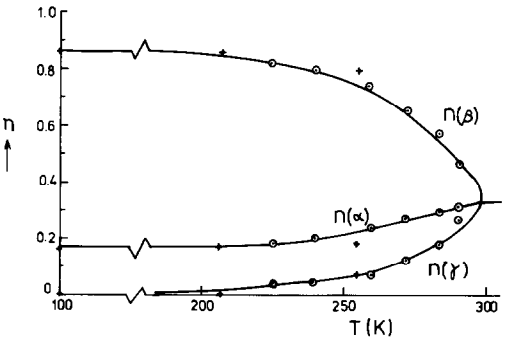


FIG. 6. Occupancies of the $\alpha$, $\beta$, and $\gamma$ sites as a function of temperature from the measurements of Section 5. The occupancies from the refinement at 255 K are included (+).

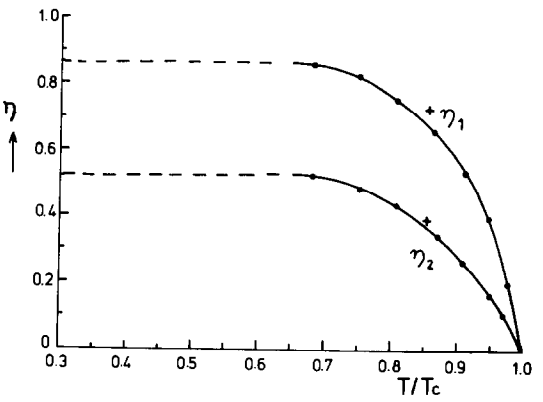


FIG. 7. The order parameters $\eta_1$ and $\eta_2$ versus $T/T_c$ calculated from the data of Fig. 6.

## 6. Bragg–Williams (Mean Field) Model for the Transition

The physical meaning of the different temperature dependencies of $\eta_1$ and $\eta_2$ is that it is more favorable to fill the $\beta$ site from the $\gamma$ site than from the $\alpha$ site. This can be understood when one writes the energy of the system in terms of nearest-neighbor repulsive interactions, $\varepsilon_1$, between silver atoms at distances $a$ (within the silver layers) and $\varepsilon_2$, between silver atoms at distance $c$ (between layers) as shown in Fig. 3.

The energy of a system of $N(\alpha) \cdot \bar{n}$ silver atoms is

$$E = 3N(\alpha)\varepsilon_1[n(\alpha)n(\beta) + n(\alpha)n(\gamma) + n(\beta)n(\gamma)] + N(\alpha) \cdot \varepsilon_2[(n^2(\alpha) + 2n(\beta) \cdot n(\gamma)]$$

where $N(\alpha)$ is the number of $\alpha$ sites, $N(\alpha) = N(\beta) = N(\gamma)$. Because the distance $c > a$, $\varepsilon_1$ will presumably be greater than $\varepsilon_2$; $\varepsilon_1$ and $\varepsilon_2 > 0$. Then it follows immediately that more energy is gained by increasing $\eta_1$ ($= n(\beta) - n(\gamma)$) than by increasing $\eta_2$ ($= (n(\beta) + n(\gamma) - 2n(\alpha))$.

Taking, for example, $n(\beta) = 0.7$, one may compare the energy $E' = E/N(\alpha)$ for two extreme cases:

(a) $n(\alpha) = 0.3$, $n(\gamma) = 0$; $E' = 0.63\ \varepsilon_1 + 0.09\ \varepsilon_2$

(b) $n(\alpha) = 0$, $n(\gamma) = 0.3$; $E' = 0.63\ \varepsilon_1 + 0.42\ \varepsilon_2$

which shows that case (a) is more favorable than (b).

The energy can be given in terms of $\eta_1$ and $\eta_2$:

$$E = N(\alpha)[3\bar{n}^2(3\varepsilon_1 + \varepsilon_2) - (\tfrac{1}{4}) \cdot (3\varepsilon_1 + 2\varepsilon_2)\eta_1^2 - (\tfrac{1}{12}) \cdot (3\varepsilon_1 - 2\varepsilon_2)\eta_2^2]$$

where $\bar{n}$ is the average occupancy of the silver sites.

In the Bragg–Williams (mean field) approximation the entropy is given by $S = k \ln W$ with

$$W = \prod_{i=\alpha,\beta,\gamma} \frac{N(i)!}{[n(i)N(i)]![(1 - n(i))N(i)]!},$$

from which one obtains, using the Sterling approximation,

$$S = -kN(\alpha) \sum_{i=\alpha,\beta,\gamma} n(i) \ln n(i) + [1 - n(i)] \ln [1 - n(i)].$$

The entropy also can be expressed in terms of $\eta_1$ and $\eta_2$. The equilibrium values of $\eta_1$ and $\eta_2$ (where $F$ has a minimum) are found from the conditions

$$\partial F/\partial \eta_1 = 0 \quad \text{and} \quad \partial F/\partial \eta_2 = 0,$$

$F$ being the free energy $F = E - TS$. The equilibrium values of $\eta_1$ and $\eta_2$ were found numerically; $\varepsilon_2$ was chosen to be $\frac{1}{3}$ of $\varepsilon_1$ and $\bar{n}$ was taken to be $\frac{1}{3}$. $F/kT$ was calculated (for a chosen value of $\varepsilon_1/kT$) as a function of $\eta_1$ and $\eta_2$ with increments of 0.01. Figure 8 shows that mean field theory predicts a second-order transition and that the temperature dependence of the order parameters is different for $\eta_1$ and $\eta_2$. The occupation probabilities of the $\alpha$, $\beta$, and $\gamma$ sites of silver as shown in Fig. 9 may be compared with those from the experiment as given in Fig. 6. Complete ordering as expected from this model is not found experimentally. Below about 200 K the ordering does not change. Intercalate order–disorder transitions of stage-1 graphite intercalates $MC_6$ were studied by a mean field model by Horie and Miyazaki (*16*). The authors took, besides the interactions $\varepsilon_1$ and $\varepsilon_2$ of our calculation, longer distance interactions into account, viz., the in-plane interactions at 2**a** + **b** (= $a\sqrt{3}$) and 2**a**, the out-of-plane interactions **a** + **c** and 2**c**. The latter interaction stabilizes a structure with three-layer ordering, *ABC*. The phase diagram showed the following transitions: *a* disordered to three-layer ordering, *ABC*, *b* disordered to two-layer ordering, *AB*, changing into three-layer ordering *ABC* at lower temperature. These possibilities depend on the ratio of the interaction energies. In our model the *AB* and *ABC* stacking would have the same free energy.

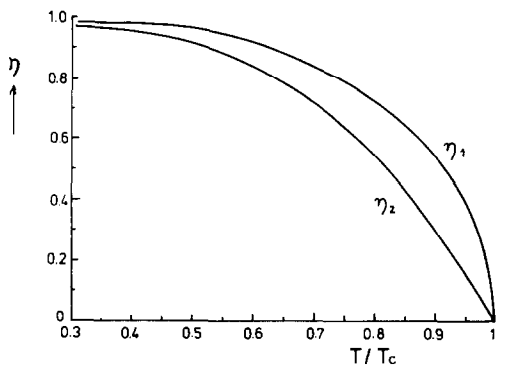


FIG. 8. The order parameters $\eta_1$ and $\eta_2$ versus $T/T_c$ from the model of Section 6. $\varepsilon_2/\varepsilon_1 = \frac{1}{3}$, $\bar{n} = \frac{1}{3}$.

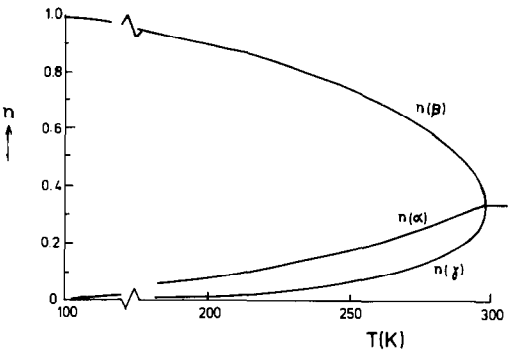


FIG. 9. Occupation probabilities of the $\alpha$, $\beta$, and $\gamma$ sites versus $T/T_c$ calculated from the data of Fig. 8.

The observation that $Ag_{0.35}TiS_2$ does not order completely (below 200 K no changes were observed) may possibly be due to the fact that a three-layer structure becomes stable. The possible transition will be of first-order character (a second-order transition is not allowed by symmetry (*13*)) and therefore kinetically slow.

The critical exponents from log $\eta$ versus log $(1 - T/T_c)$ plots using data of the model are 0.5 and 1.0 for $\beta_1$ and $\beta_2$, respectively. The values from the experiments are between those predicted by Bak (*15*) and those from mean field theory. For both models the energy depends on nearest-neighbor interaction only. In the Bragg–Williams approximation the entropy is calculated assuming that the occupancy of, e.g., an $\alpha$ site depends only on the average of the occupancy of the $\alpha$ sites; in Bak's model the entropy is calculated exactly but with the same assumption as for the energy. Our experimental data suggest that interactions of longer distance than nearest neighbors must be taken into account.

The mean field approximation used in the 2D $a\sqrt{3} \times a\sqrt{3}$ order–disorder transition, taking $\bar{n} = \frac{1}{3}$ and $n(\alpha) = n(\gamma) \neq n(\beta)$ (the $\alpha$ and $\gamma$ sites now being equivalent), does not lead to a second-order transition. We found $\varepsilon/kT_c$, where the order parameter jumps from $\eta = 0.275$ to $\eta =$ in a first-order way, to be 1.4675. This value of $\varepsilon/kT_c$ is in agreement with that given by Osorio and Falicov (*17*) in the mean field calculation of the phase diagram ($\varepsilon/kT_c$ versus composition). These authors also calculated the phase diagram in the triangle approximation, $\varepsilon/kT_c$ for $\bar{n} = \frac{1}{3}$ now being 2.77. First-order character of the 2D $a\sqrt{3} \times a\sqrt{3}$ transition using the Bethe–Peierls approximation for the entropy was found by Campbell and Schick (*18*).

We investigated the character of the 3D order–disorder transition for some values of the ratio $q = \varepsilon_2/\varepsilon_1$. For $q = 0.1$ we found first-order character; for $q = 0.25$ the character changed to second order.

It may be noted that $\varepsilon/kT_c$ from mean field theory deviates considerably from those using more accurate expressions for the entropy. Following the methods of the cluster variation method, $T_c$ may differ as much as a factor of 2.

An approach similar to the one given here, but also including the variation in composition, was used by Oka *et al.* (*19*) for the order–disorder transitions of phases $V_3S_4$ and $V_5S_8$ with monoclinic superstructures of the $Cd(OH)_2$ type subcell. Calculated occupation probabilities of interlayer vanadium atoms against temperature plots for the transition of the $V_3S_4$ to $Cd(OH_2)$ structure show the same trends as observed for $Ag_{0.35}TiS_2$. The same phenomenon as found by us, viz., first-order character of the transition when the interlayer interaction is small, was also calculated by Oka *et al.* (*19*) for the $V_3S_4$ and $V_5S_8$ to $Cd(OH)_2$ transition. Experimental data concerning the occupation probabilities versus temperature in the case of $V_3S_4$ and $V_5S_8$ are, however, not available.

## 7. The Ordered Structure in (3 + 1)D Superspace

The ordered structure can be considered to be a commensurately modulated structure with vector $\mathbf{q} = \frac{1}{3}\mathbf{a}^* + \frac{1}{3}\mathbf{b}^* + \frac{1}{2}\mathbf{c}^*$. Consequently a (3 + 1)-dimensional superspace group (de Wolff *et al.* (*20*) can be determined which describes the symmetry of the modulated phase (*21*). In the reciprocal unit cell of the substructure all reflections can be described by

$$\mathbf{s}^* = h\mathbf{a}^* + k\mathbf{b}^* + 1\mathbf{c}^* + m\mathbf{q},$$

$m = \pm 1, \pm 2, 3$ being the order of the satellites. Reflections with $m = 0$ correspond to the subcell reflections. Due to the commensurately, $m$ is restricted to $-3 < m \leq 3$. The relation between satellite reflections in the description of a modulation and the type of reflection in 3D reciprocal space can easily be deduced from Fig. 10. First-order satellites ($m = \pm 1$) correspond to reflections $HKL$ with $H - K \neq 3n$, $L$ odd in 3D space. Second-order satellites correspond to reflections with $H - K \neq 3n$, $L$ even in 3D space.

An interesting feature is noticed for the

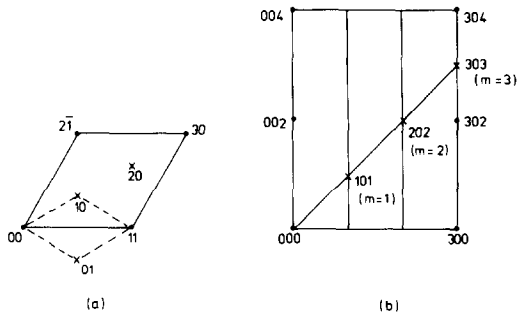


FIG. 10. (a) Reciprocal lattice plane ($a^*b^*$ plane); dots and crosses correspond to subcell and superreflections (with indices *HKL*). (b) The section through reciprocal space, $m = 1, 2, 3$, indicates the first-, second-, and third-order satellites, respectively, of 000.

third-order satellites. Third-order satellites correspond to reflections *HKL* with $H - K = 3n$ (including *HHL*) with $L$ odd in 3D space. Reflections *HHL* with $L$ odd are the extinct reflections in space group $P\bar{3}1c$; reflections $H - K = 3n$, $H \neq K$, with $L$ odd are all allowed in space group $P\bar{3}1c$. For satellites one expects the intensities on the average to decrease in the order $m = 1$ to 3. Superreflections with $L$ even ($m = 2$) are indeed found weaker than those with $L$ odd ($m = 1$). It was observed that a number of forbidden reflections in $P\bar{3}1c$ are present with intensities exceeding $3\sigma(I)$. This means that the true symmetry is $P3$ or $P\bar{3}$ rather than $P\bar{3}1c$, the deviation from $P\bar{3}1c$ being small. The allowed reflections in $P\bar{3}1c$, *HKL* with $H - K = 3n$ ($n \neq 0$) and $L$ odd have about the same intensities (some exceeding $3\sigma(I)$) as the forbidden reflections *HHL* with $L$ odd. In 3D description they are weaker because silver atoms do not contribute. In (3 + 1)D space all reflections, *HKL*, $H - K = 3n$, and $L$ odd are weak because they are third-order satellites. The observations are in agreement with the (3 + 1)D superspace group described in the $a\sqrt{3} \times a\sqrt{3} \times 2c$ supercell to be $T^{P\bar{3}m1}_{\bar{1}\bar{1}\ 1}$. It may be noted that this space group does not occur in the list of (3 + 1)D superspace groups of de Wolff *et al.* (*20*). It belongs to a new Bravais class, which applies only to some particular commensurately modulated structures (van Smaalen (*21*)).

We therefore conclude that a superspace group description explains the observed peculiarities of the diffraction pattern in a more natural way then the conventional description in 3D space.

The function describing the modulation consists of two parts: an occupational modulation for silver and a displacive modulation for sulfur and titanium. The occupational modulation function gives the same intensity function for first- and second-order satellites as the conventional method for superreflections with $L$ odd and even in $P\bar{3}1c$. A full account will be given elsewhere (*22*).

## 8. Related Phases

$Li_xTiS_2$ ($0 < x < 1$), at room temperature isostructural with disordered stage-1 $Ag_xTiS_2$ and $Li_xTaS_2$ with a lithium sublattice similar to that of $Li_xTiS_2$, has been the subject of a large number of studies. A review of structures and properties and new results were described recently by Dahn and McKinnon (*23*). So far no direct experimental evidence from neutron- or X-ray diffraction is available for the existence of 3D order–disorder transitions as found for $Ag_{0.35}TiS_2$.

Trigonal $Cr_2S_3$ ($Cr_{1/3}[CrS_2]$) and $Cr_5S_6$ ($Cr_{2/3}[CrS_2]$) are isostructural with ordered $Ag_{0.35}TiS_2$; Cr atoms occupy $\frac{1}{3}$ of the available octahedral sites between sandwiches $CrS_2$ in the case of $Cr_2S_3$, and $\frac{2}{3}$ of these sites in the case of $Cr_5S_6$. Both ordered phases with unit cells $a\sqrt{3} \times a\sqrt{3} \times 2c$ have space group $P\bar{3}1c$ (*24*). As discussed in Section 4, one may expect second-order phase transitions to a disordered structure with $a \times a \times c$ unit cell space group $P\bar{3}1c$. One also expects the transitions to occur at

a higher temperature than found for $Ag_{0.35}TiS_2$ because of the higher charge of the ions involved ($Cr^{3+}$) and the absence of shielding ($Cr_2S_3$ and $Cr_5S_6$ are semiconductors; $Ag_{0.35}TiS_2$ is a metal). Experimentally it was found for trigonal $Cr_2S_3$ that the order persists up to at least 1150 K. $Cr_5S_6$ shows a peritectic decomposition at about 600 K into the disordered phase and $Cr_3S_4$ (*25, 26*).

The same type of sublattice order as found for $Ag_{0.35}TiS_2$ is present in phases $M_{1/3}TX_2$ ($M$ is a 3D transition element, $T$ = Nb, Ta; $X$ = S, Se). $M$ atoms occupy $\frac{1}{3}$ of the available octahedral sites between sandwiches $TX_2$ which have the metal $T$ in trigonal–prismatic coordination. In the ordered structure, space group $P6_322$ (*27*), as well as in the assumed disordered structure, the unit cell contains two units $TX_2$ in the direction of the $c$-axes. The order–disorder transition will be from a structure with a $a\sqrt{3} \times a\sqrt{3} \times c$ unit cell, space group $P6_322$, to a structure with $a \times a \times c$ unit cell, space group $P6_3/mmc$. So far no order–disorder transitions have been reported.

## Acknowledgment

We thank Professor Haas for critically reading the manuscript.

## References

1. G. A. Scholz and R. F. Frindt, *Mater. Res. Bull.* **15,** 1703 (1980).
2. R. M. Suter, M. W. Shafer, P. M. Horn, and P. Dimon, *Phys. Rev. B: Condens. Matter* **26,** 1495 (1982).
3. A. G. Gerards, H. Roede, R. J. Haange, B. A. Boukamp, and G. A. Wieger, *Synth., Met.* **10,** 51 (1984–1985).
4. M. Mori, K. Oshima, S. C. Moss, R. F. Frindt, M. Plischke, and J. C. Irwin, *Solid State Commun.* **43,** 781 (1982).
5. M. Plischka, K. K. Bardhan, R. Lionelli, and J. C. Irwin, *Canad. J. Phys.* **61,** 397 (1983).
6. K. I. Oshima and S. C. Moss, *Acta Crystallogr. Sect. A* **39,** 298 (1983).
7. A. Lionelli, M. Plischka, and J. C. Irwin, *Phys. Rev. Lett.* **45,** 1291 (1980).
8. J. L. de Boer and A. Duisenberg, "Enraf–Nonius CAD4F Diffractometer Software Update, Groningen and Utrecht, The Netherlands, February 1984."
9. A. L. Spek, "Proceedings of the 8th European Cryst. Meeting," Liege, Belgium (1983).
10. J. M. Stewart, P. A. Machin, C. Dickinson, H. Ammon, L. Heck, and H. Flack, "The X-ray 76 system," Technical Report TR 446, Computer Science Center, University of Maryland, Collegepark, MD.
11. D. T. Cromer and J. B. Mann, *Acta Crystallogr. Sect. A* **24,** 321 (1968).
12. G. A. Wiegers, H. J. M. Bouwmeester, and A. G. Gerards, *Solid State Ionics* **16,** 155 (1985).
13. C. Haas, *Solid State Commun.* **4,** 419 (1966).
14. C. Haas, private communication.
15. P. Bak, *Phys. Rev. Lett.* **44,** 889 (1980).
16. C. Horie and H. Miyazaki, *Canad. J. Phys.* **63,** **64** (1985).
17. R. Osorio and L. M. Falicov, *J. Phys. Chem. Solids* **43,** 73 (1982).
18. C. E. Campbell and M. Schick, *Phys. Rev. A* **5,** 1919 (1972).
19. Y. Oka, K. Kazuga, and S. Kachi, *J. Solid State Chem.* **24,** 41 (1978).
20. P. M. de Wolff, A. Janner, and T. Jansen, *Acta Crystallogr. Sect. A* **37,** 625 (1981).
21. S. van Smaalen, Thesis, Groningen (1985).
22. S. van Smaalen, K. D. Bronsema, and G. A. Wiegers, to be published.
23. J. R. Dahn and W. R. McKinnon, *J. Phys. C* **17,** 4231 (1984).
24. F. Jellinek, *Acta Crystallogr.* **10,** 620 (1957).
25. C. F. van Bruggen, Thesis, Groningen (1969).
26. T. J. A. Popma and C. F. van Bruggen, *J. Inorg. Nucl. Chem.* **31,** 73 (1969).
27. K. Anzenhofer, J. M. van de Berg, P. Cossee, and J. N. Hell, *J. Phys. Chem. Solids* **31,** 1057 (1970).